

Exposure of Cross-linked Epoxy Resins to the Space Environment*

A. GARTON,[†] P. D. McLEAN, W. WIEBE, and R. J. DENSLEY,
National Research Council of Canada, Ottawa, Ontario, K1A 0R6

Synopsis

Two specimens of cross-linked epoxy resins were attached to the Remote Manipulator Arm ("Canadarm") of the space shuttle and exposed to the space environment (about 225 km altitude) experienced on the 41-G shuttle mission. Portions of the specimens which had been coated with 10 nm of inconel, then gold, were relatively unaffected by space exposure, while the uncoated areas were eroded to a depth of about 5 μm . The eroded surfaces had a porous texture, consisting of tunnel-like features extending a further 10 μm below the surface, with a hole density of 3×10^6 holes/ mm^2 . Surface infrared (IR) spectroscopy showed that the first 1–2 μm of porous surface material was little affected chemically by the erosion process, indicating that any chemical erosion must have occurred progressively in a very thin surface layer, which then volatilized away, exposing fresh surface for attack. As a qualitative laboratory simulation, specimens of the same plastics were exposed to low-pressure air and oxygen plasmas. Somewhat similar surface damage was observed, with no IR-detectable change in surface chemistry. The criteria for selection of a satisfactory laboratory simulation of the space environment, and the factors responsible for the directionality of the erosion processes are discussed.

INTRODUCTION

Cross-linked epoxy resins are used as the matrix component of many advanced composite materials. Such materials are finding increasing use in structural and aerospace applications, where their high specific stiffness and ease of fabrication offer unique design advantages over metals. As part of a continuing program to evaluate and improve organic matrices for advanced composites, two specimens of cross-linked epoxy resins were exposed to the space environment experienced on shuttle mission 41-G (October 1984). One specimen contained an example of an "epoxy fortifier," a recently developed class of additives which improve the physical and mechanical properties of amine-cured epoxy resins.^{1,2} Portions of the specimens received a thin (~ 10 nm) metallic coating to determine the effectiveness of this mode of protection against the low Earth orbit environment.

Many organic materials have been shown to suffer a loss of surface integrity when exposed to the low Earth orbit environment.^{3–7} This effect is generally attributed to chemical erosion by atomic oxygen, which is facilitated by the high contact energies (~ 5 eV) for atomic collisions with forward-facing spacecraft components. The specimens described here were chosen for orbital exposure both to broaden our understanding of the erosion processes (most of

* Issued as NRCC No. 25966.

[†] To whom correspondence should be addressed.

the data in the open literature refer to polyimide and polyester films), and for the practical reason that cross-linked epoxy resins are likely to find increasing use as the matrix component of composite materials for long term use in space.

EXPERIMENTAL

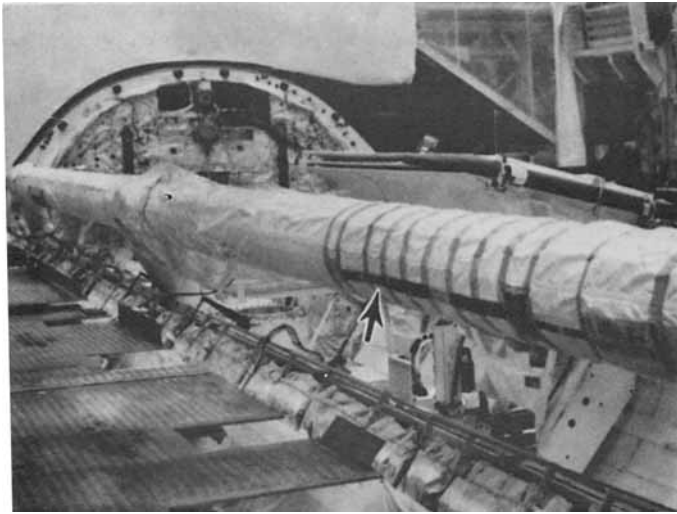
Description of Specimens

Specimen I was prepared from an epoxy resin (XD 7818, Dow Chemical, the diglycidyl ether of bisphenol F, 100 parts) and an aromatic amine curing agent (Tonox, Uniroyal, a mixture of metaphenylene diamine and methylene dianiline, 22.5 parts). Specimen IV was made using the same resin (100 parts) but it also contained an epoxy fortifier (Fortifier C, made by Uniroyal Ltd., Chemicals Division of Elmira, Ontario, Canada, formulation proprietary) at a level of 30 parts and a higher level of curing agent than Specimen I (34.5 parts Tonox). The ingredients were degassed, mixed at 100°C, and poured into stainless steel moulds. The cure cycle was five hours at 80°C, two hours at 125°C, and four hours at 175°C. Standard tensile test specimens made from these materials had strengths of 98 MPa (I) and 122 MPa (IV), tensile moduli of 3100 MPa (I) and 3800 MPa (IV), and elongations of 6.0% (I) and 5.5% (IV). Specimen IV also showed the ductile failure mode characteristic of fortified epoxy resins.^{1,2} The glass transition temperatures were 160°C (I) and 142°C (IV).

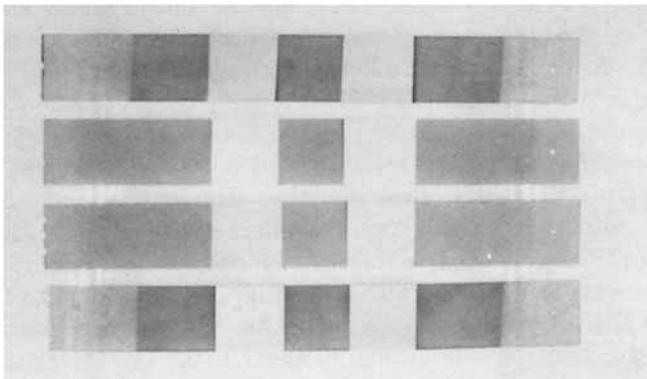
The moulded sheets (17.8 × 10.2 × 0.32 cm) were cut into bars 15.2 × 1.91 cm and machined on both sides to remove traces of mould release agent and to meet the mission-specified thickness requirement of 1.1 mm. The machined specimens were given partial metallic coatings, 1.9 cm square, to provide protected sections of the plastic for reference after exposure. The coating procedure was to wash the machined specimens with water, then isopropanol, before drying in argon. The specimens were then heated in vacuum to 150°C and a gold film applied over an inconel (a nickel alloy) intermediate layer to a total thickness of about 10 nm.

The two specimens were attached to the exterior surface of the Canadarm at a position 217 cm from the wrist, 109.5° to the arm Y axis, and in the axial direction (Fig. 1). Double-sided Kapton tape fixed the samples side by side. Nylon thread was fed through holes in each specimen and tied around the circumference of the arm. Finally, single-sided Kapton tape was wrapped around the circumference of the arm to cover the ends of each specimen (see Fig. 1 and CRC drawing M13, 747-E Aug. 7, 1984, available on request).

Because of their location, the specimens experienced a range of orientations relative to the ram direction (i.e., the direction of the flight, which is not necessarily coincident with the direction in which the front of the spacecraft points). The majority of the exposure time was accumulated with the specimens oriented normal to the ram direction. From a knowledge of the position of the arm boom at the other times, off-normal exposure time could be corrected to an equivalent normal exposure time by a geometric correction for the reduced atomic flux at off-normal orientations. In such a way it was estimated that the specimens experienced the equivalent of 38 hours of normal



(a)



(b)

Fig. 1. (a) Plastic specimen mounted on the Canadarm for the 41-G Shuttle mission. (b) Space-exposed and nonexposed specimens in sequence (top to bottom) I (exposed), I (unexposed), IV (unexposed), IV (exposed).

ram exposure at an altitude of 225 km. The only other manipulator operation which resulted in appreciable exposure of specimens to the ram direction was a series of "water dumps."⁸ In this case one edge of Specimen I was approximately facing the ram direction for at least 10 hours. The specimens were protected in the cargo bay during take off and re-entry.

Specimen Characterization

The specimens for examination by scanning electron microscopy (SEM, Bausch and Lomb "Novascan") were gold coated in the conventional fashion to reduce charging in the electron beam. Surface replicas for transmission electron microscopy (TEM, Phillips 201) were made using a two-stage cellulose acetate-carbon process.

The infrared (IR) spectrum of the first 1–3 μm (depending upon wavelength) of the plastic surface was examined by internal reflection spectroscopy (IRS) using a KRS-5 IRS element (Harrick Scientific Corp., Ossining, NY). The roughness of the surface limited optical contact between the specimen and the IRS element. However, adequate contact could be produced if a moderate compressive force was placed on the IRS assembly (30 in. oz torque on the screws of the IRS sample holder described in Ref. 9), although this reduced the useful lifetime of the soft IRS element.

Laboratory Simulations

Attempts were made to simulate in a qualitative sense the aggressive environment of low Earth orbit by exposing specimens to air and oxygen plasmas in the laboratory. The initial attempt at simulation involved the use of a conventional laboratory plasma cleaner (Harrick Scientific) to provide a radio frequency (rf)-induced plasma (5 W energy dissipation) in a tubular reactor under flowing atmospheres of air or oxygen at 10^{-2} to 0.4 Torr. A parallel plate-type reactor was also constructed with one electrode powered by an rf supply (up to 200 V at 27 MHz) with the sample sitting on the grounded electrode. Such a system is capable of producing ions of higher kinetic energy than with the plasma cleaner, because of the higher accelerating potential, and is sometimes called "reactive ion sputtering."¹⁰

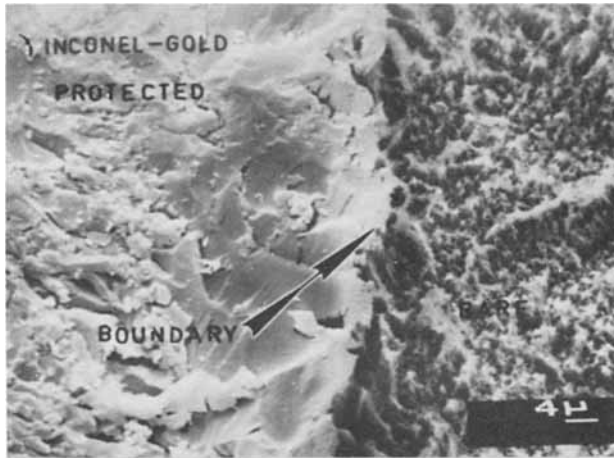
To investigate the effect of surface charging on the erosion processes, a localized electric field was induced in some specimens before exposure to the plasma. A specimen equivalent to IV, but with polished surfaces, was heated to 160°C (i.e., higher than its glass transition temperature) and subjected to a dc electrical potential of 20 kV/cm. The effect of the electric field is to align the dipoles in the sample and to inject space charges. The specimen was then cooled to room temperature with the potential still applied, thus freezing into position the aligned dipoles and space charges.¹¹ Such a specimen then exerts its own electric field and is known as an electret (the electrical equivalent of a magnet). The magnitude of the weight loss during exposure to a plasma and the eroded surface morphology can then be compared for electrets and identical uncharged specimens.

RESULTS

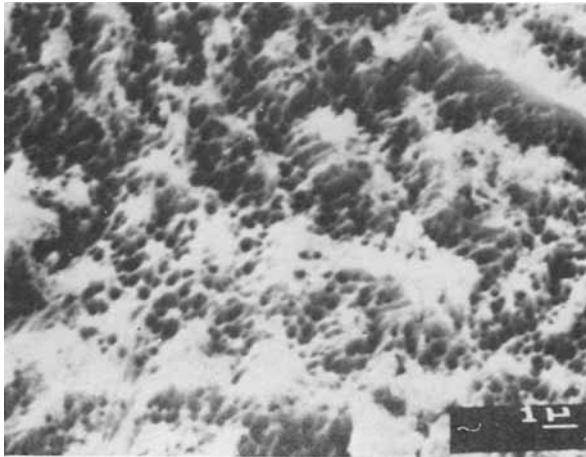
Examination of Space-Exposed Specimens

Visually, the space-exposed specimens were slightly darker in color than the unexposed controls and the uncoated portions of the specimens had a "frosted" appearance (Fig. 1). Both visually and by microscopic examination the effects of space exposure were indistinguishable between the top surfaces of Specimens I and IV, and so results presented below for one specimen can be considered as typical of both. However, the edges of the specimens were not equivalent because of the unique exposure history of the outer edge of Specimen I (see Experimental section).

Figure 2(a) shows the boundary between the protected and unprotected areas of the top surface of Specimen I. The surface roughness of the protected area resulted from the specimen machining and was identical to that on the



(a)

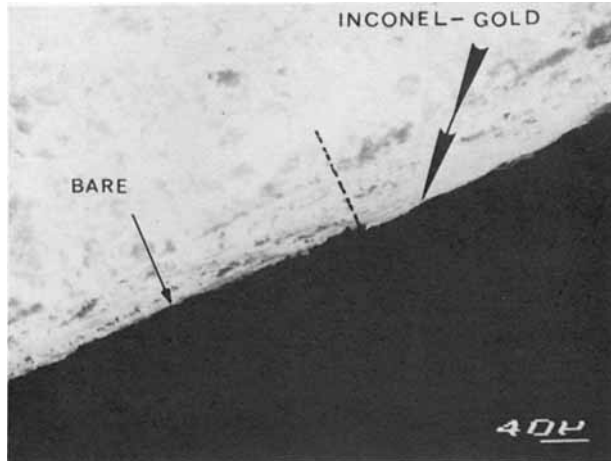


(b)

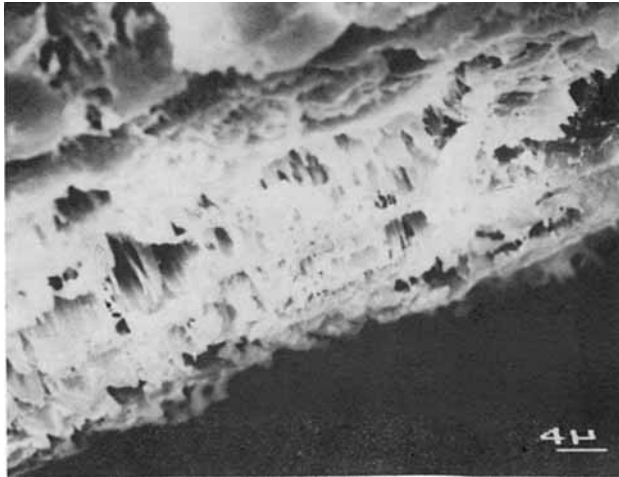
Fig. 2. (a) Comparison of inconel-gold protected area with unprotected area for space-exposed Specimen I. (b) Porous texture of the unprotected area of space-exposed Specimen I.

control specimen. Figure 2(b) shows the unprotected area at higher magnification and it is evident that the damaged surface contains numerous holes. An estimate of the "density" of holes is of the order of 3×10^6 holes/mm². The diameter of the holes range from 0.2 to 0.3 μ m.

An examination of the edge of Specimen I in the region of the boundary between the gold-coated and unprotected areas showed the presence of a "step," indicating a loss of material from the unprotected area of the top surface to a depth of about 5 μ m [Fig. 3(a)]. Further, at higher magnification [Fig. 3(b)], the edge of Specimen I appeared damaged to a depth of several microns, with tunnel-like features oriented roughly normal to the edge surface.



(a)

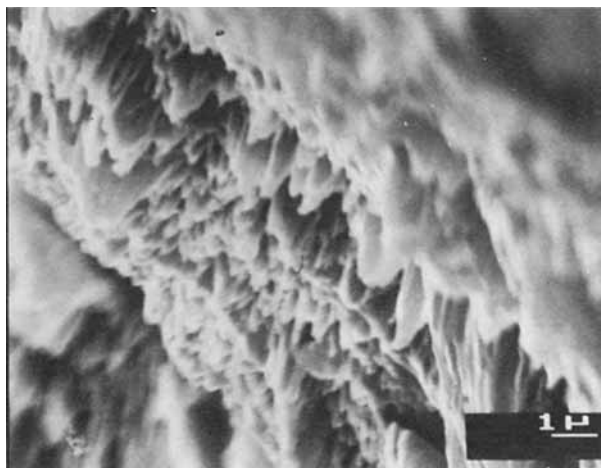


(b)

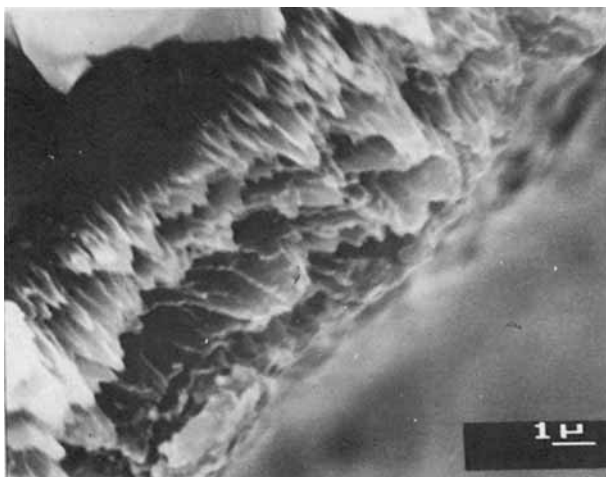
Fig. 3. (a) Erosion and material damage on the edge of space-exposed Specimen I. (b) Tunneling on the edge of the space-exposed Specimen I in the unprotected area.

Figure 4 shows that, at least in a qualitative sense, the damage on the unshielded edge of Specimen I was similar in form to the damage on the top surface. A high angle of incidence was used to obtain the micrographs shown in Figure 4, so as to highlight the depth of the tunneling in both eroded surfaces.

One edge of Specimen I was partially shielded from the space environment because the two specimens were mounted in contact side by side on the arm boom (Fig. 1). Figure 5 shows a comparison of the two edges of Specimen I. The protected edge [Fig. 5(b)] has a surface texture identical to the original machined edge. The exposed edge [Fig. 5(a)] shows that the original surface structure was completely destroyed and replaced with a porous structure



(a)

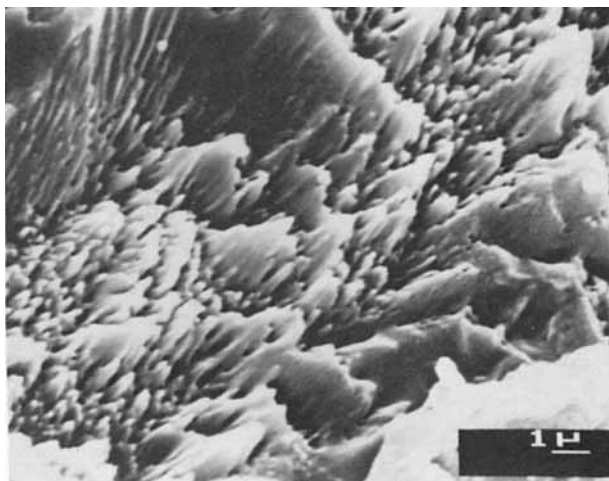


(b)

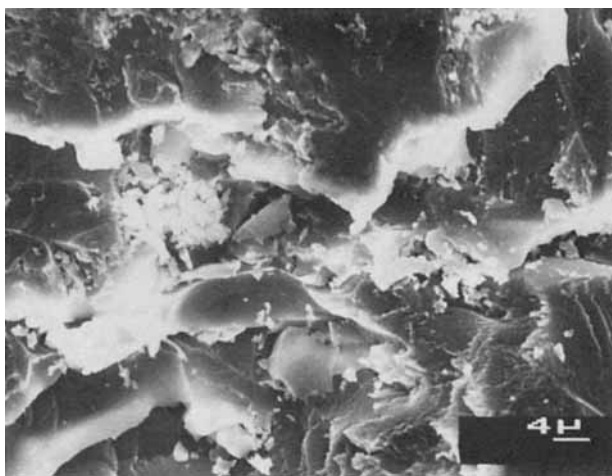
Fig. 4. A comparison of edge and to surfaces of space-exposed Specimen I. (a) Edge. (b) Top.

similar to that seen on the top surface. The micrographs in Figure 5 were obtained at approximately normal incidence and so demonstrate well the diameter of the tunnel-like features on the surface ($\sim 0.3 \mu\text{m}$). Both edges of Specimen IV appeared relatively undamaged.

In order to obtain further information about the nature of the tunneling observed on the surfaces of the specimens, a transverse notch was cut along the unexposed side of Specimen I and the specimen was then fractured, thereby exposing a section through the space-damaged material. This fracture sectioning revealed the extent of the depth of the tunneling, and that



(a)



(b)

Fig. 5. A comparison of exposed and unexposed edges of space-exposed Specimen I. (a) exposed. (b) unexposed.

individual tunnels varied in depth and diameter (Fig. 6). The average diameters of the tunnels corresponded well with the diameters of the holes observed on the surface of the specimen [Fig. 2(b)].

Examination in the TEM of two stage replicas of the specimen surface provided more information on the morphology of the tunnel. Figures 7(a) and 7(b) confirm that the tunnels are circular in cross-section, and that their maximum diameters are of the order of 0.2 to 0.3 μm . Other features of interest are the apparently flat circular forms at the bottom of the tunnels and some evidence of circular and in some cases apparent spiral markings on the walls of the tunnels [arrows, Fig. 7(a)].

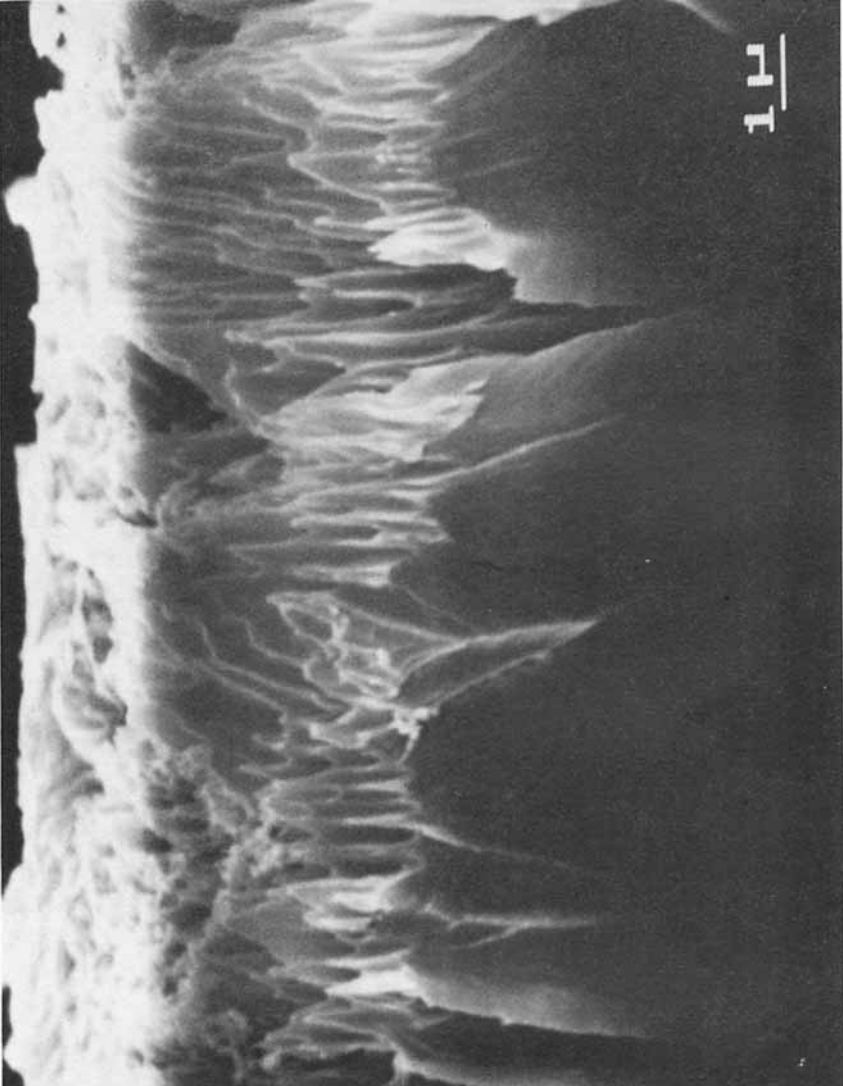


Fig. 6. Surface degradation due to tunneling as observed on fracture section of space-exposed Specimen I (unprotected area).



Fig. 7. TEM of surface replica from unprotected top surface of space exposed Specimen I.

Figure 8 shows that the chemical nature of the first 1–2 μm of the eroded surface of Specimen I was relatively unchanged by space exposure, as evidenced by its IR spectrum, despite the presence of appreciable surface damage to a depth of at least 10 μm . If oxidation had occurred in this surface layer, it would have been apparent as a characteristic absorption at about 1720 cm^{-1} . Note, however, that this surface had a porous texture and obviously no

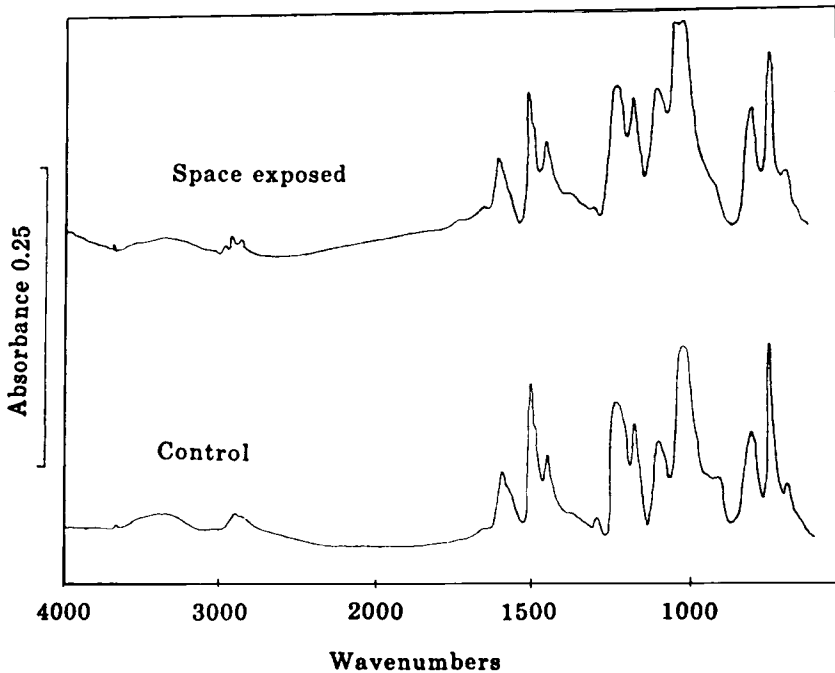


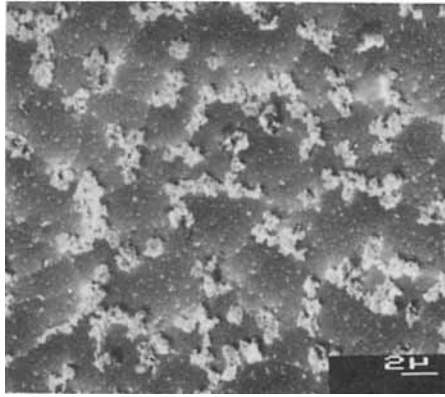
Fig. 8. IRS spectra of surface of Specimen I.

comment can be made on the chemical state of the material which has been removed, only on that which remains.

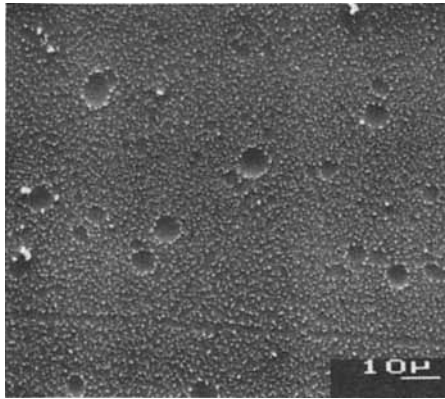
Examination of Laboratory-Exposed Specimens

The abilities of various laboratory-generated plasmas to erode cross-linked epoxy resins were compared in a semiquantitative fashion, so as to allow us to develop a testing procedure to assist in the selection of materials and protective coatings for future space exposure. No attempt was made to develop a realistic low Earth orbit simulator, which would require much more precise control of the variables of pressure, temperature, and gas energetics. Instead we wished only to rank materials and coatings in their ability to withstand an aggressive environment which has some qualitative similarities to the low Earth orbit environment. The specific features of the space-erosion processes which we attempted to duplicate in the laboratory were the localized nature of the erosion (tunneling) and the apparent absence of redeposition of eroded material.

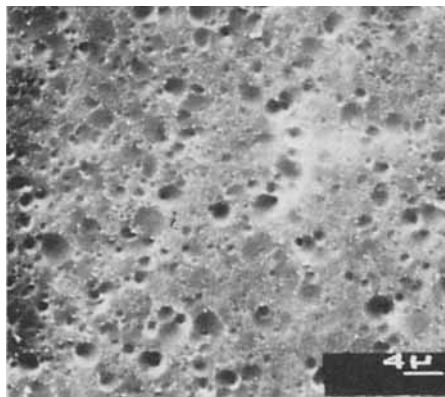
Figure 9 shows examples of the surface modifications which can be produced by exposure of polished specimens to rf-induced plasmas in the cylindrical reactor. Low pressures of oxygen ($\leq 10^{-2}$ Torr) and a low rate of gas flow over the sample encourage redeposition of the eroded material as is shown in Figure 9(a). Higher pressures of oxygen (10^{-1} Torr) and a higher rate of gas flow reduce the amount of apparent redeposition and produce some localization of the erosion processes [Fig. 9(b)]. Substitution of air for oxygen as the plasma medium produced the least apparent redeposition of eroded material



(a)



(b)



(c)

Fig. 9. SEM of plasma-treated Specimen IV (tubular reactor). (a) Oxygen at $\leq 10^{-2}$ Torr; (b) oxygen at 10^{-1} Torr; (c) air at 10^{-1} Torr.

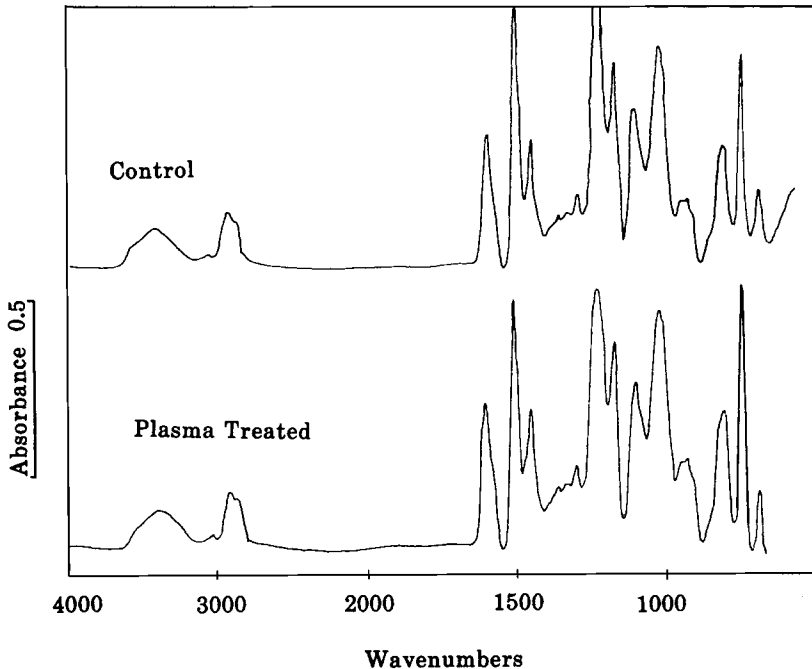
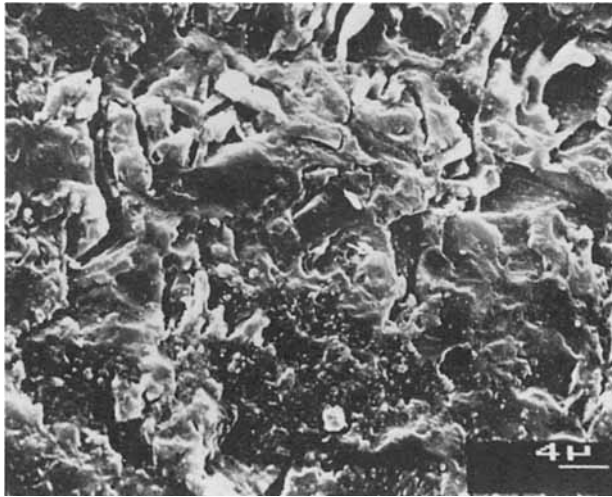


Fig. 10. IRS spectra of surface of plasma-treated Specimen IV (air plasma, 10^{-1} Torr, 17 h exposure).

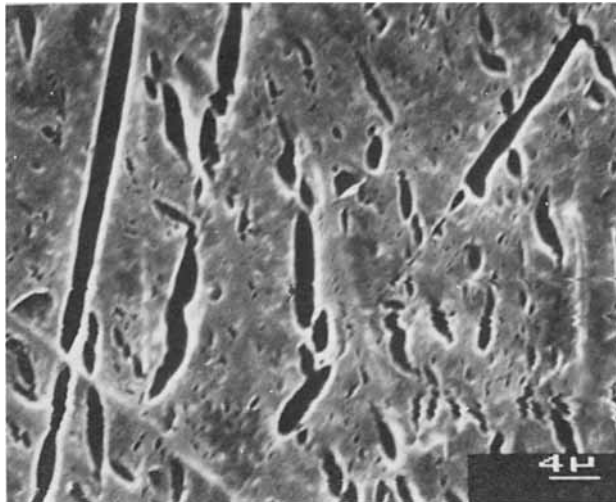
and the erosion was in the form of localized pitting of about $1\ \mu\text{m}$ diameter and up to $1\ \mu\text{m}$ in depth [Fig. 9(c)]. IR spectroscopy of the surface $1\text{--}2\ \mu\text{m}$ of the air plasma-exposed specimen (Fig. 10) showed that, as with the space-exposed specimen (Fig. 8), extensive surface damage was not associated with appreciable chemical modification of the uneroded residue. This observation confirms that the erosion processes must be highly localized and the eroded material is removed by volatilization, so exposing fresh surface to attack.

Exposure of the electrically charged specimen (see Experimental section) to an air plasma, in the cylindrical reactor, showed that the effect of electrical charging was to increase the rate of erosion under otherwise identical conditions. After 17 h in the rf-induced air plasma, the electret suffered twice the weight loss (4.65%) as an identical uncharged specimen (2.4%).

The use of a parallel plate reactor allows the production of more highly energetic charged species than with the cylindrical reactor because of acceleration of ions and electrons toward the electrodes. At high power dissipations (20 W), this results in catastrophic disruption of the specimen surface, some of which may be caused by localized heating [Fig. 11(a)]. Sputtering of the metal electrodes can also occur, resulting in deposition of copper on the specimen and on the walls of the reactor. At low power dissipations (5 W), the erosion was in the form localized pitting and cracking [Fig. 11(b)]. The erosion also was highly nonuniform over the sample as a whole and frequently was concentrated at defects on the original specimen.



(a)



(b)

Fig. 11. SEM of plasma-treated Specimen I (parallel plate reactor): (a) 20 W power dissipation in air at ~ 0.3 Torr; (b) 5 W power dissipation, in air at ~ 0.4 Torr.

DISCUSSION

The two questions addressed below are the nature of the erosion processes in low Earth orbit, and the criteria for selection of a laboratory test method for screening materials and coatings for space application.

The environment experienced by the orbiting shuttle may be considered as a low-density plasma, whose characteristics will change markedly with altitude, time of day, and solar activity.¹² The major neutral species at these altitudes

is atomic oxygen at a typical density of 7×10^{14} atoms. m^{-3} . The major ionic species is O^+ (at typical daytime values of 2.5×10^{11} ions. m^{-3}) accompanied by electrons with energies equivalent to 4000–5000°K. The chemical activity of these reactive species will be further enhanced by the velocity of the spacecraft, which leads to high interaction energies at surfaces facing the ram direction (e.g., ~ 5 eV for oxygen atom/surface interactions). In addition, any electrical charging of the surfaces will modify the local plasma environment and provide high kinetic energies to reactive ions in the plasma.

Atomic oxygen is well known to be capable of eroding polymer surfaces and has been proposed as the major source of deterioration of organic and some optical materials in low Earth orbit. Total oxygen fluxes on surfaces (obtained from knowledge of their surface orientation, atomic oxygen levels, and the flight characteristics) have been calculated to be in the order of 10^{20} atoms/ cm^2 of surface. It is therefore reasonable to conclude that atomic oxygen makes a significant contribution to the erosion of surfaces facing the ram direction. The apparent protection by a 10 nm layer of gold (Fig. 2) is also consistent with this explanation because metal surfaces are known to catalyze the recombination of atomic oxygen to molecular oxygen. However, the microscopic evidence of Figures 2–7 also leads us to speculate on what other processes are involved in the erosion phenomenon.

The most noticeable microscopic feature we report here is the occurrence of tunnels, up to 10 μm long and about 0.3 μm diameter, in both the top and exposed edge of the specimens. One initial speculation was that the tunneling represented some morphologic feature in the plastic which was exposed by preferential erosion. However, no such morphology could reasonably be expected to occur in both specimens and we also have evidence for similar features on the surface of exposed polyimide film,¹³ i.e., material with a very different inherent morphology. Tunneling via individual particle collisions (e.g., with dust particles) also seems unlikely because of the ability of ~ 10 nm of gold to provide protection (Fig. 2).

The occurrence of the tunneling phenomenon on the top surfaces of both specimens and on only one edge of Specimen I clearly indicates an association with exposure to the ram direction. Several mechanisms can be postulated for the localization of the erosion in the form of tunnels. The combination of ~ 5 eV translational energy and the chemical reactivity of the atomic species in low Earth orbit is sufficient to cause molecular scissions, and finally volatilization, in the polymer surface layer. From a knowledge of the atomic oxygen flux and the extent of mass loss for polyester and polyimide films, Leger et al.³ calculated that the rate of erosion was about 3×10^{-24} cm^3 /atomic oxygen collision, which represents a very low efficiency of scission reactions per collision. It is conceivable that the yield of molecular scissions per reaction may be higher at a defect than on a flat area of the surface. Such an effect may result from multiple collisions with the surface before reflection of the atoms, or from easier loss of scission products by volatilization. The product would be localized erosion, eventually resulting in tunnels. This is somewhat analogous to the production of "sputter cones" on bombardment of surfaces with high energy ions,¹⁰ although it should be noted that ion energies associated with sputter cone formation (several thousand eV) are appreciably higher than the translational energies accessible to atomic oxygen.

Another mechanism which deserves attention is the possibility of surface charging providing very high kinetic energies to ionic species (particularly O^+) in the low Earth orbit environment. The electrical charging of spacecraft has been of concern for many years, particularly for spacecraft in geosynchronous Earth orbit, where electrical discharges can cause the breakdown of insulating materials and interfere with the functioning of electronic components. In low-Earth orbit the plasma is colder and denser than in geosynchronous orbit and so passive charging from the plasma is likely to be less important. However, specimen charging is possible through inductive effects, high energy radiation, or triboelectric effects and may vary with location on the spacecraft. Clearly, for the space-exposed samples, only a moderate amount of surface charging would be necessary to give O^+ ions, although they are few in number, much higher kinetic energies than neutral species impinging on the ram facing surfaces. The localization of the erosion processes then occurs because the sputter yield (i.e., the number of atoms ejected per incident bombarding ion) can be higher at a defect than on the flat portions of the specimen.¹⁰ The use of different plasma-generation conditions (Figs. 9, 11) certainly demonstrate that the energies of the plasma modify the course of the erosion processes but, not unexpectedly, it was not possible to duplicate exactly the eroded surface structure of the space-exposed specimens. The higher mass loss from the electrically charged specimens in the laboratory plasma also indicates that electrical effects may be important.

Whatever the chemical species responsible, the erosion process is limited to a thin surface layer. Presumably, sufficient polymer backbone scission occurs to allow the degraded material to be volatilized away, so exposing fresh surface for attack. The absence of any significant chemical modification of even the first 1–2 μm of surface (Figs. 8, 10) indicates that uniform degradation of the specimen does not occur.

It was not possible to duplicate exactly the detailed nature of the surface erosion in the space-exposed specimens by laboratory plasma exposure. This is not surprising in view of the fact that the plasma environment of the spacecraft will be continually changing with time of day, attitude, and orientation of the specimens. The selection of laboratory plasma conditions for materials testing will therefore be somewhat arbitrary and largely determined by practical restrictions. However, criteria for the selection of a testing procedure may be summarized:

1. Redeposition of eroded material must be avoided: this can be achieved by having the maximum gas flow rate over the sample consistent with the chosen pressure and available pumping capacity.
2. As large an area of uniform plasma environment should be available: this is best achieved in a tubular reactor surrounded by an rf coil.
3. Excessive sample heating and/or sputtering of the reactor walls must be avoided: the lowest power dissipation consistent with reasonable erosion rates should be used.
4. The atmosphere should be at least a reasonable simulation of that encountered in practice: flowing air at low pressure was chosen, although the choice of pressure is affected by the requirement of rapid gas flow (see No. 1).

Such a procedure is intended only as a means of obtaining a relative ranking of material resistance to aggressive environments and is not meant to be a realistic laboratory simulation of the low-Earth orbit environment. On the basis of such a laboratory test program it is planned to select further cross-linked epoxy resins and protective coatings better able to withstand space exposure and to test these materials on future shuttle flights.

We wish to thank Dr. D. G. Zimcik of the Communications Research Centre, Ottawa, Ontario, for his invaluable assistance in coordination of arrangements for exposure of the specimens on the 41-G shuttle mission. We also wish to thank Dr. G. A. Dobrowolski and Mr. M. A. Waldorf of NRC, Division of Physics, for the inconel-gold coating of the specimens.

References

1. P. D. McLean, A. Garton, R. F. Scott, and S. E. Gransden, U. S. Patent 4,480,082.
2. P. D. McLean, R. F. Scott, and A. Garton, *Br. Polym. J.*, **15**, 66 (1983).
3. L. J. Leger and J. T. Visentine, Proc. American Institute for Aeronautics and Astronautics, 22nd Aerospace Sciences Meeting, Reno, Nevada, Jan. 9–12, 1985, Preprint A1AA-84-0548.
4. A. F. Whitaker, *NASA Technical Memorandum*, TM-86463 (1984).
5. P. N. Peters, R. C. Linton, and E. R. Miller, *J. Geophys. Res.*, **10**, 569 (1971).
6. L. J. Leger, *NASA Technical Memorandum*, TM 58246 (1982).
7. R. C. Tennyson, J. B. French, L. J. Kok, J. Kleiman, and D. G. Zimcik, Proc. American Institute for Aeronautics and Astronautics, 13th Space Simulation Conference, Orlando, Florida, Oct. 8–11, 1985, NASA Conference Publication CP-2340.
8. M. Garneau (Canadian Payload Specialist), private communication.
9. D. J. Carlsson and D. M. Wiles, *Can. J. Chem.*, **48**, 2397 (1970).
10. B. Chapman, *Glow Discharge Processes*, Applied Science Publishers, New York, 1980.
11. P. Hedvig *Dielectric Spectroscopy of Polymers*, Wiley, New York, 1977.
12. J. V. Iribarne and H. R. Cho, *Atmospheric Physics*, D. Reidel Publishing, New York, 1980.
13. W. Wiebe, unpublished results.

Received December 31, 1985

Accepted February 16, 1986